Environmental Research Letters

CORRIGENDUM

Corrigendum: The role of precipitation type, intensity, and spatial distribution in source water quality after wildfire (2015 *Environ. Res. Lett.* **10** 084007)

Sheila F Murphy[1], **Jeffrey H Writer**[1,2], **R Blaine McCleskey**[1] **and Deborah A Martin**[1]

[1] US Geological Survey, 3215 Marine Street, Boulder, CO 80303, USA
[2] University of Colorado, Boulder, CO 80309, USA

E-mail: sfmurphy@usgs.gov

OPEN ACCESS

RECEIVED
18 April 2016

ACCEPTED FOR PUBLICATION
16 June 2016

PUBLISHED
8 July 2016

The original article (Murphy *et al* 2015 *Environ. Res. Lett.* 10 084007) contained an incorrect map of rainfall intensity in figure 5(c). The correct version of figure 5 is shown below. The correct data were used in the analyses, and thus this error has no bearing on the interpretation of the data and conclusions.

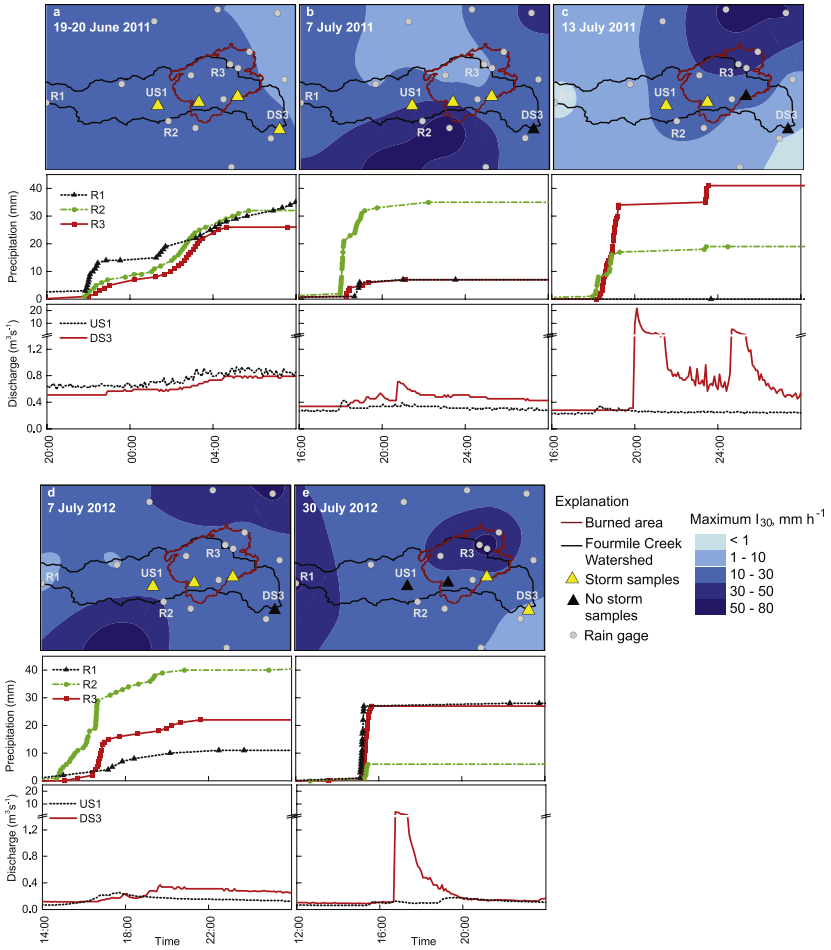

Figure 5.

Environmental Research Letters

LETTER

The role of precipitation type, intensity, and spatial distribution in source water quality after wildfire

Sheila F Murphy[1], **Jeffrey H Writer**[1,2], **R Blaine McCleskey**[1] **and Deborah A Martin**[1]

[1] US Geological Survey, 3215 Marine Street, Boulder, CO 80303, USA
[2] University of Colorado, Boulder, CO 80309, USA

E-mail: sfmurphy@usgs.gov

Keywords: wildfire, forests, water quality, landscape disturbance, rainfall intensity, climate change, North American Monsoon

Supplementary material for this article is available online

OPEN ACCESS

RECEIVED
13 February 2015

REVISED
2 July 2015

ACCEPTED FOR PUBLICATION
3 July 2015

PUBLISHED
7 August 2015

Abstract

Storms following wildfires are known to impair drinking water supplies in the southwestern United States, yet our understanding of the role of precipitation in post-wildfire water quality is far from complete. We quantitatively assessed water-quality impacts of different hydrologic events in the Colorado Front Range and found that for a three-year period, substantial hydrologic and geochemical responses downstream of a burned area were primarily driven by convective storms with a 30 min rainfall intensity >10 mm h^{-1}. These storms, which typically occur several times each year in July–September, are often small in area, short-lived, and highly variable in intensity and geographic distribution. Thus, a rain gage network with high temporal resolution and spatial density, together with high-resolution stream sampling, are required to adequately characterize post-wildfire responses. We measured total suspended sediment, dissolved organic carbon (DOC), nitrate, and manganese concentrations that were 10–156 times higher downstream of a burned area compared to upstream during relatively common (50% annual exceedance probability) rainstorms, and water quality was sufficiently impaired to pose water-treatment concerns. Short-term water-quality impairment was driven primarily by increased surface runoff during higher intensity convective storms that caused erosion in the burned area and transport of sediment and chemical constituents to streams. Annual sediment yields downstream of the burned area were controlled by storm events and subsequent remobilization, whereas DOC yields were closely linked to annual runoff and thus were more dependent on interannual variation in spring runoff. Nitrate yields were highest in the third year post-wildfire. Results from this study quantitatively demonstrate that water quality can be altered for several years after wildfire. Because the southwestern US is prone to wildfires and high-intensity rain storms, the role of storms in post-wildfire water-quality impacts must be considered when assessing water-quality vulnerability.

1. Introduction

About half of the water supply for the southwestern US states of Arizona, Colorado, New Mexico, and Utah is derived from forested land (Brown *et al* 2008). Water supply from forested land is generally of higher quality, and thus less expensive to treat for human consumption, than that derived from any other land use. Not only are fewer pollutants present, but forest cover reduces flooding from storms (Dudley and Stolton 2003), which are important drivers of suspended and dissolved constituents to surface water (Williams 1989, Inamdar and Mitchell 2006, Raymond and Saiers 2010). However, forests are vulnerable to wildfire: more than 5.1 million ha of land have burned in these states (4.7% of total area) since 1984 (based on areas burned at low, moderate, or high severity; Wildland Fire Research Council's Monitoring Trends in Burn Severity website, www.mtbs.gov), including important forested surface-water supply watersheds (figure 1(a)). Wildfires increase susceptibility of watersheds to flooding and erosion and thus

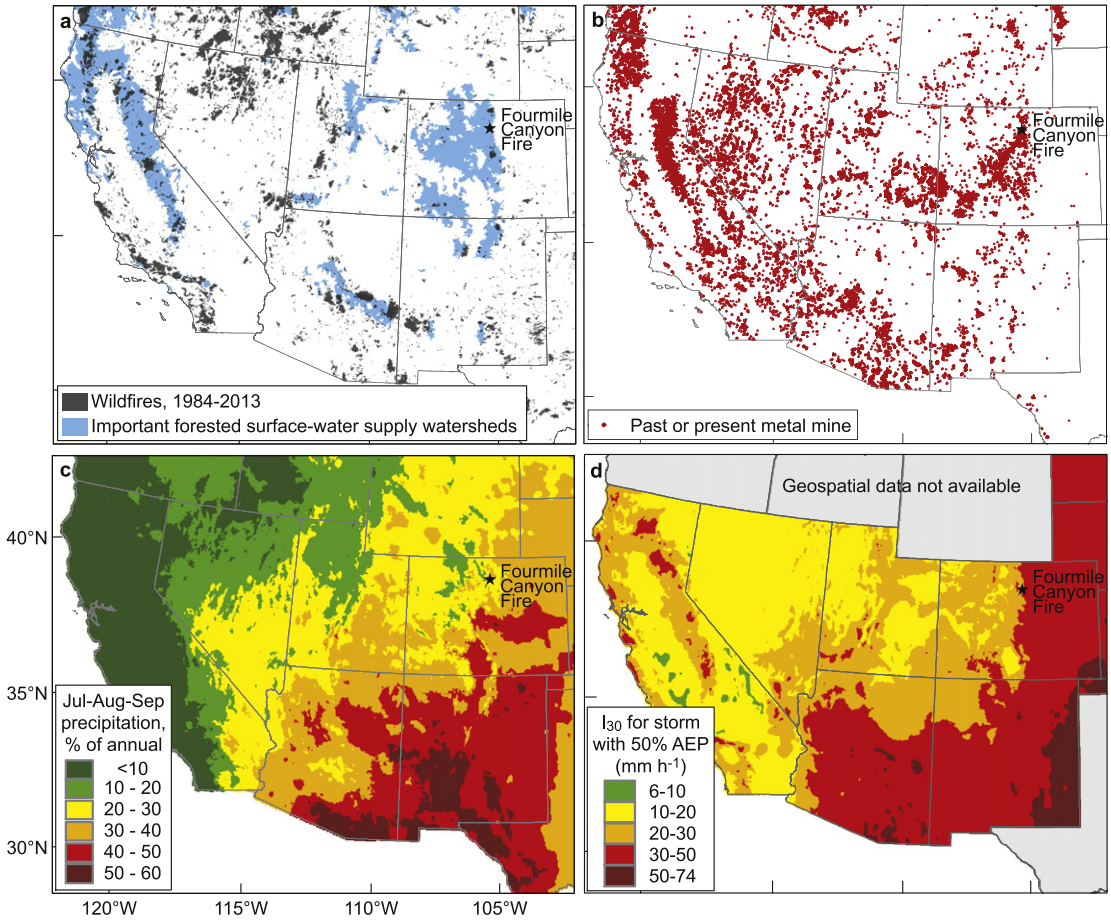

Figure 1. Maps of the southwestern US, showing (a) important forested surface-water supply watersheds (based on population served and intake locations, weighted by percent forest; Weidner and Todd 2011) and wildfires from 1984–2013 (www.mtbs.gov), (b) past or present metal mines (http://mrdata.usgs.gov); (c) percent mean annual precipitation contributed July–September, 1981–2010 (http://prism.oregonstate.edu), and (d) 30 min rainfall intensity (I_{30}) in mm h^{-1} for storm with 50% annual exceedance probability (AEP; Perica *et al* 2013).

can have both short- and long-term impacts on water supplies, such as increased treatment costs, need for alternative supplies, and diminished reservoir capacity (Smith *et al* 2011). Post-wildfire runoff and erosion has recently impaired the water supplies of Denver, Albuquerque, and other southwestern US cities (Morton *et al* 2003). A compounding factor in the southwestern US is the abundance of easily erodible waste from historical mining and milling (figure 1(b)); wildfires may leave these sites vulnerable to increased surface runoff and erosion.

Post-wildfire runoff and erosion are most severe during high-intensity rainfall (Moody *et al* 2013). Therefore, water supplies from wildfire-prone forests that receive high-intensity rainfall are at substantial risk of wildfire-induced water-quality impairment. In the southwestern US, wildfire activity is greatest from May–July (Barbero *et al* 2014), and up to 60% of annual precipitation is delivered in July–September (figure 1(c)), largely in response to the North American Monsoon and Great Plains convection (Adams and Comrie 1997, Higgins *et al* 1997). Thus, newly burned areas have little time to recover before the onset of high-intensity rainfall, which occurs relatively frequently: in most of the southwestern US, rain storms with 30 min rainfall intensity (I_{30}) 20–74 mm h^{-1} have a 50% annual exceedance probability (AEP; Perica *et al* 2013) (figure 1(d)). Surface runoff can occur in recently burned forest in the region when $I_{30} > 10$ mm h^{-1} (100% AEP; Moody and Martin 2009).

Because post-wildfire water-quality impairment is greatest in response to storms (Smith *et al* 2011), high-frequency discharge and water-quality measurements are critical to quantifying fluctuations, maximum constituent concentrations, and yields. We previously demonstrated substantial increases in turbidity, total suspended solids (TSS), dissolved organic carbon (DOC), and nitrate (NO_3^-) concentrations downstream of a burned area in response to convective storms ten months after wildfire (Murphy *et al* 2012, Writer *et al* 2012, Writer and Murphy 2012). The objective of this study, which expands temporally to 3.3 years post-wildfire (encompassing both drought and a rainstorm that delivered more than half of the average annual precipitation to the burned area), is to quantitatively assess the role of rainfall intensity on stream concentrations and yields of constituents that

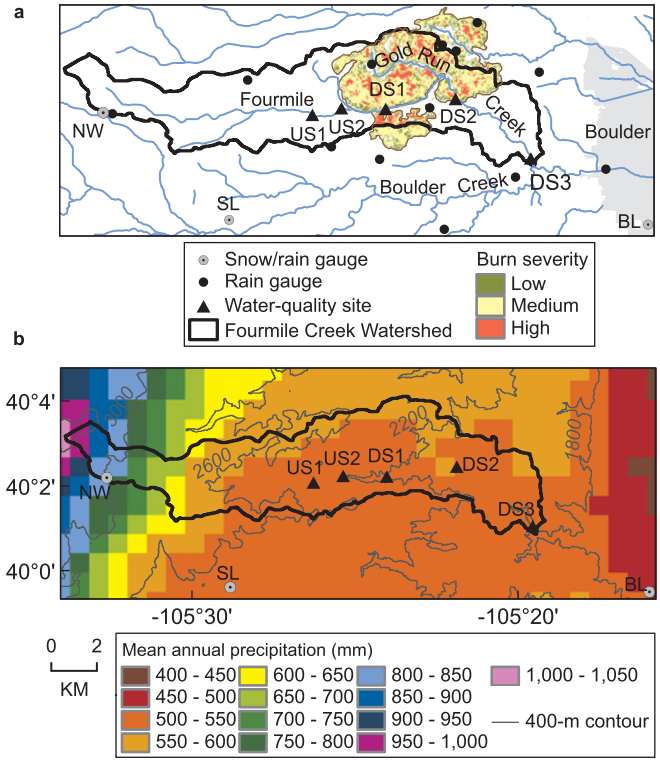

Figure 2. Maps of the Fourmile Creek Watershed, showing (a) burn severity for the Fourmile Canyon Fire (low, differenced Normalized Burn Ratio (dNBR) 84–117; medium, 118–195; high, dNBR 196–255) (www.mtbs.gov), precipitation gages, and sampling sites and (b) mean annual precipitation (1981–2010; http://prism.oregonstate.edu) and 400 m elevation contour intervals.

are often elevated post-wildfire (Emelko *et al* 2011, Bladon *et al* 2014) and can impair water treatability (Crittenden *et al* 2012): TSS, NO_3^-, DOC, and manganese (Mn). We evaluate rainfall data with high temporal resolution (minutes) from a dense network (1 rain gage per 17 km^2) to determine spatially explicit rainfall intensity, its relation to a burned area, and the resulting sediment and chemical export. We also assess altered seasonality of hydrological and chemical export.

2. Study area

The 2370 ha Fourmile Canyon fire burned 23% of the 6330 ha Fourmile Creek watershed, Colorado at mixed burn severity in September 2010 (figure 2(a)). We sampled Fourmile Creek at sites upstream (US1 and US2) and downstream (DS1, DS2, DS3) of the burned area with similar geology (metamorphic and granitic rocks), pre-fire land cover (77–79% forest, 16–19% shrubland/grassland, <1% developed), and mean basin slope (33–37%) (table S1). Historical (1860s–1940s) mining of gold, tungsten, and other metals left tailings and waste rock dispersed throughout the watershed (Murphy 2006) and areas disturbed by mining and related logging have been revegetating for 70 years or more. Mean annual precipitation (MAP) is 500–600 mm in the burned area and at the study sites, but much higher in the headwaters of Fourmile Creek; west of 2600 m elevation, MAP increases ~50 mm per 100 m elevation to 1000 mm (figure 2(b)). As in most post-wildfire studies, pre-wildfire water quality data are limited, and due to variations in elevation ranges, headwater area, land cover, and historical land use in nearby watersheds, there is no ideal exterior reference watershed. However, our upstream sites have similar geology, land cover, and historical mining activity, and therefore serve well as unburned reference watersheds.

3. Methods

Daily precipitation totals and type were obtained from three stations near the Fourmile Creek watershed that record both snow and rain (figure 2(a); data for BL from www.esrl.noaa.gov/psd/boulder, SL from http://nadp.sws.uiuc.edu, and NW from www.wcc.nrcs.usda.gov). We also obtained incremental rainfall data from 1.0 mm tipping-bucket rain gages operated by the Urban Drainage and Flood Control District (UDFCD; https://udfcd.onerain.com/home.php). For the period June through September (when precipitation is typically in the form of rain), we calculated daily rainfall totals for these gages, and when daily rainfall exceeded 10 mm at three UDFCD gages in or near the burned area (or at SL or BL), we determined I_{30}. Maps of maximum I_{30} during storms were produced using a Geographic Information System (GIS) (universal kriging, exponential semivariogram, variable search radius).

Stream discharge (5 min) at sites DS2 and DS3 was obtained from USGS stream-gaging stations (06727500 and 06727410; http://waterdata.usgs.gov/nwis), which operated April–September. Water-level loggers were deployed to monitor stage at sites US1 and DS1 (and at DS2 and DS3 in 2011 prior to installation of stream gages) every 5 min for the same period, and stream discharge was measured periodically to develop rating curves for discharge estimation (Rantz *et al* 1982).

Water-quality grab samples were collected monthly or semi-monthly during base-flow conditions (October–February), and 2–8 times monthly from March–September (frequency decreased in second and third years as knowledge was gained about the system). Samples were collected at more frequent intervals (0.3–4.0 h) during and after precipitation events with automatic samplers, which began sampling when stream stage reached an actuator or when the sampler was manually started. Actuators were set to 5–7 cm above water level during routine visits; due to constantly changing stage during snowmelt runoff, the actual height above water may have been higher or lower when triggered. During some storms, upstream stage response to storms was too small to initiate automatic sampling, or downstream samplers became clogged and would only sample part (or none) of the event. Samples were delivered within 6 h of collection (for routine samples) and 24 h of collection (for storm samples) to the USGS National Research Program laboratory in Boulder, CO. Samples were filtered through a 0.40- or 0.45 μm membrane filter and preserved as required for the analysis of the constituent (as described in (McCleskey *et al* 2012). A subset of unfiltered samples was acidified with nitric acid and filtered through a 0.45 μm membrane filter for 'total recoverable' cations. Concentrations of major cations and trace metals were determined using inductively coupled plasma–optical emission spectrometry. Nitrate concentrations were determined by ion chromatography. Concentrations of DOC were measured by wet oxidation. Additional details, along with quality assurance/quality control information, are available in McCleskey *et al* (2012). Water-quality data are provided in the SI.

Turbidity of unfiltered samples was measured within 4 h of collection for routine samples and 48 h of collection for storm samples using a turbidimeter. If a sample exceeded the maximum range of the turbidimeter (1000 nephelometric turbidity units (NTU)), it was diluted with deionized water, agitated, and re-analyzed with the turbidimeter. TSS concentrations were determined for a subset of samples (McCleskey *et al* 2012), and TSS was estimated from turbidity using a simple linear regression (Murphy *et al* 2012). We excluded samples with turbidity <3 NTU and/or TSS < 3 mg L^{-1} from the regression due to a poor relationship at such low values. For samples with turbidity <800 NTU (the highest turbidity standard we used, and for which no sample dilution was required), we used the regression TSS = 1.166 × turbidity + 2.84 ($r^2 = 0.75$), while for samples with turbidity >800 NTU we used the regression TSS = 1.479 × turbidity − 98 ($r^2 = 0.85$). (These regressions differ slightly from those reported in Murphy *et al* (2012) due to inclusion of three years of data and removal of low-turbidity samples from the regression).

Statistical evaluation of differences in constituent concentrations at upstream and downstream sites was performed with the Kruskal–Wallis test (Hollander and Wolfe 1999). Daily DOC and dissolved Mn loads (in kg d^{-1}) were determined using the Load Estimator (LOADEST) program (Runkel *et al* 2004) using average daily discharge and measured concentrations unless more than three samples were collected in a day (due to a storm event); in that case, daily load was calculated by integration. The LOADEST program was not used for TSS, NO_3^-, or total recoverable Mn load calculations due to poor correlation of concentrations with discharge. Rather, daily NO_3^- loading was calculated by multiplying measured concentration by average daily discharge (NO_3^- values were interpolated between samples); if more than one NO_3^- value was available in one day, average NO_3^- was used. We calculated loads using both 0 and the detection limit (0.03 mg NO_3^- L^{-1}) for samples that were below detection; the difference in annual loading was between <1 and 5% at sites DS1, DS2, and DS3, and between 3 and 22% at US1. We report the average of these two methods. The same method was used to calculate daily TSS loads for September–May; however, since TSS changed by orders of magnitude during storms, discharge and TSS were each interpolated to one-minute intervals for June–August (and September 2011). If automatic samplers began sampling well into an event and/or ended prior to the end of the event, the previous or following grab sample was used for TSS prior to or after the event. This method was used to avoid grossly overestimating TSS. If downstream automatic samplers did not sample (as on July 13, 2011 due to clogging of sampler intakes at DS2 and DS3 by debris), minimum loads were estimated from upstream sites. When estimated TSS was <6 mg L^{-1}, we calculated loads using both 0 and 6 mg L^{-1}; the difference in annual loading was between <1% and 19% at DS1, DS2, and DS3, and between 8 and 47% at US1. We report the average of these methods. Total recoverable Mn (which includes dissolved, colloidal, and any particulate matter that would pass through a 0.45 μm filter after acidification) was analyzed for only a subset of samples, but concentrations were very well correlated with measured TSS (total Mn = 0.0045 × $TSS^{0.8324}$; $r^2 = 0.940$), so we estimated monthly total recoverable Mn loads from TSS loads. Because not all storms were sampled (due to clogging of the sampler intake or the river stage not rising to the level of automatic sampler actuator), we consider our load estimates to be minimum values. Seasonal and annual

runoff values were calculated by dividing stream discharge by drainage area, and seasonal and annual yield (t ha^{-1} or kg ha^{-1}) by dividing load by drainage area.

Extensive flooding in September 2013 caused substantial infrastructure damage (including loss of stream gages and data loggers, and impassable roads), so for access and safety reasons discharge and water-quality measurements were limited for the rest of that year. We estimated runoff and minimum TSS load at DS3 for September from four samples (discharge was estimated from UDFCD stream gages on Boulder Creek upstream and downstream of Fourmile Creek).

4. Results and discussion

4.1. Rainfall intensity and spatial distribution drive stream response after wildfire

The greatest hydrological and water-quality impacts for three years after the Fourmile Canyon fire were observed in response to summer storms, when maximum concentrations downstream of the burned area were 120 000 mg TSS L^{-1}, 12 mg NO_3^- L^{-1}, 71 mg DOC L^{-1}, 2.2 mg Mn L^{-1} (dissolved), and 110 mg Mn L^{-1} (total recoverable) and exceeded levels that affect water treatment (Crittenden *et al* 2012) by several orders of magnitude (figure 3, table S2). These concentrations were 31, 14, 10, 156, and 153 times greater, respectively, than maximum upstream concentrations during storm events. Grouping of geochemical data into four categories of maximum precipitation intensity 12 h prior to sampling (0, 1–10, 11–30, and 31–55 mm h^{-1}) reveals that median and/or maximum TSS, NO_3^-, DOC, and Mn concentrations at the downstream sites increased with increasing I_{30}, and were significantly higher when $I_{30} > 10$ mm h^{-1} (figure 4; table S2). Water-quality impairment was greatest when $I_{30} > 30$ mm h^{-1} (50% AEP). In contrast, DOC, NO_3^-, and Mn concentrations at the upstream site (US1) did not change or increased only slightly as I_{30} increased, even when $I_{30} > 30$ mm h^{-1}, and median concentrations remained below water-treatment thresholds. Upstream TSS concentrations increased with increasing I_{30}, but median TSS was <200 mg L^{-1} at all I_{30} categories. Lower rainfall intensity thresholds were required to export constituents downstream of the burned area; for example, when I_{30} was 1–10 mm h^{-1}, downstream TSS, DOC, and dissolved and total recoverable Mn concentrations were statistically similar to upstream concentrations when $I_{30} > 10$ mm h^{-1} (figure 4).

Higher rainfall intensity, and therefore impaired water quality at downstream sites, was a seasonal phenomenon: during the 3.3 years of this study, 22 of 24 days with $I_{30} > 10$ mm h^{-1} and all 7 days with $I_{30} > 30$ mm h^{-1} (50% AEP or less) fell in July–September (figure 3). Spring frontal storms (e.g. 18–19 May 2011 and 19–20 June 2011) had similar or greater daily rainfall, were larger in areal extent, and had lower spatial variability in rainfall total and intensity than convective storms, but much lower maximum I_{30} (figure 5, table S3). These events produced a smaller downstream response in discharge and TSS, NO_3^-, and DOC concentrations than convective storms, and no difference in dissolved Mn concentrations (figure 3).

The geographic distribution of rainfall intensity relative to the burned portion of the Fourmile Creek Watershed was an important determinant of post-wildfire hydrologic response and water quality. For example, on 30 July 2012, rainfall with $I_{30} > 30$ mm h^{-1} fell both upstream and within the burned area; discharge downstream of the burned area increased 42 times (figure 5(e)) and we observed the highest TSS concentrations recorded during the study. Upstream discharge increased by only 2.9 times (and did not reach a level required to trigger automatic samplers). The spatial distribution of rainfall *within* the burned area was also an important factor in hydrologic and geochemical response, and demonstrates the need for a dense rain gage network. On 7 July 2011, maximum I_{30} recorded at the three rain gages in the burned area was 12 mm h^{-1} (table S3), but interpolation with gages outside of the burned area suggested that maximum I_{30} in the southern part of the burned area was 30–40 mm h^{-1} (figure 5(b)), which was confirmed by independent rain gages in the area (Moody and Ebel 2014). Peak discharge on 7 July 2011 (0.71 m^3 s^{-1}) was much less than on 13 July 2011 (22 m^3 s^{-1}), when high-intensity rainfall was focused on the steep, 70% burned Gold Run subwatershed (figures 2(a) and 5(c)). The 7 July event resulted in maximum concentrations of 31 000 mg TSS L^{-1}, 51 mg DOC L^{-1}, 9 mg NO_3^- L^{-1}, and 0.35 mg dissolved Mn L^{-1} at site DS2 (figure 3). Sampler intakes at DS2 and DS3 were clogged with sediment and burned debris on 13 July so we cannot directly compare geochemical response, but black, sediment-laden water was videorecorded at site DS2 and in Gold Run. Extensive erosion of mine waste along a Gold Run tributary was observed, and much greater sediment deposition was observed in the channel and stream banks after that storm. Thus, we suspect TSS concentrations were substantially higher on 13 July than on 7 July. Two storms in 2012 with $I_{30} > 30$ mm h^{-1} (5 July 2012 and 30 July 2012; the latter is shown in figure 5(e)) fell in the Gold Run subwatershed and again led to high discharge and impaired water quality (figure 3).

Altered post-wildfire watershed response during and after storm events is evident not only by comparing sites upstream and downstream of the burned area, but to historical discharge data. Published water-quality data prior to 2010 are limited to six samples in 1975, 1977, 1985, and 2000 that were collected in June, September and October (Murphy *et al* 2003). Concentrations of TSS, NO_3^-, DOC, and Mn concentrations were similar to those we observed during the same periods prior to July 2011 storms; none of these

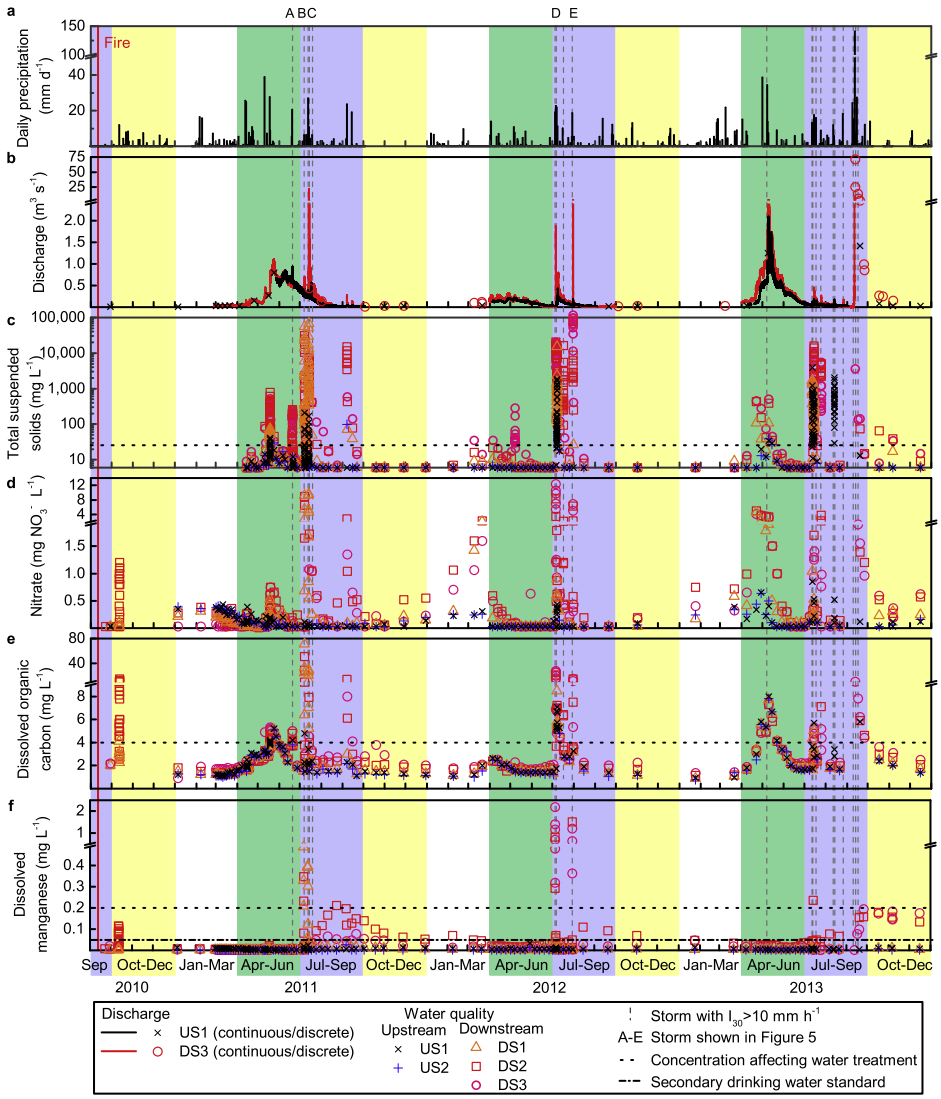

Figure 3. (a) Daily precipitation (at site SL for October–May (no data available for 1–24 January 2011, 31 October–5 November 2012, or 6 November–2 December 2013) and average of three rain gages in burned area for June–September). (b)–(f) Stream discharge and constituent concentrations in Fourmile Creek (note that US2 was not instrumented for storm sampling). Storms with $I_{30} > 10$ mm h^{-1} identified with dashed verticals, and letters indicate storms evaluated in figure 4. Levels affecting water treatment (horizontal dashed lines) are based on turbidity of 20 nephelometric turbidity units (equivalent to 26 mg L^{-1} total suspended sediment in this study) and 4 mg L^{-1} dissolved organic carbon, above which conventional treatment, rather than filtration, is typically required, and both 0.2 mg L^{-1} manganese, above which growth of microorganisms in reservoirs and distribution systems can be promoted, and 0.05 mg L^{-1}, the secondary drinking water standard established by the US Environmental Protection Agency (Crittenden *et al* 2012).

samples were collected during storms, so we cannot compare the water-quality response during storm events. Analysis of historical discharge data, however, showed that the highest peak annual discharge at site DS3 prior to the wildfire (22 y of record) was 7.3 m^3 s^{-1}, recorded on both 6 June 1949 and 1 June 1991 (figure 6). A rain gage at R3 (figure 2(a)) received 87 mm rainfall on 31 May–1 June 1991, the second highest 2-day total in 23 y; maximum I_{30} was 42 mm h^{-1} (https://udfcd.onerain.com/home.php). Peak discharge in 2011, the first year after the Fourmile Canyon fire, was three times greater than in 1991 (22 m^3 s^{-1} on 13 July; the highest 15 min discharge, to match frequency of historical data, was 9.6 m^3 s^{-1}), despite lower rainfall (50 mm on 12–13 July 2011 at RS3) and similar maximum I_{30} (42 mm h^{-1}). Higher post-fire peak discharge has been attributed to altered hydrologic conditions that favor overland or near-surface flow, such as decreased interception (Neary *et al* 2005), loss of surface cover (Larsen *et al* 2009), decreased evapotranspiration (Dore *et al* 2012), and changes to soil hydraulic properties (Moody *et al* 2013). Greater overland flow can lead to increased transport of ash and sediment to streams after wildfire (Smith *et al* 2011). Overland flow and entrained debris was observed on burned hillslopes within the Fourmile Creek watershed (Moody and Ebel 2014, Moody and Martin 2015) during the storms when we measured water-quality impairment. We infer that overland flow was greater after the wildfire, compared to

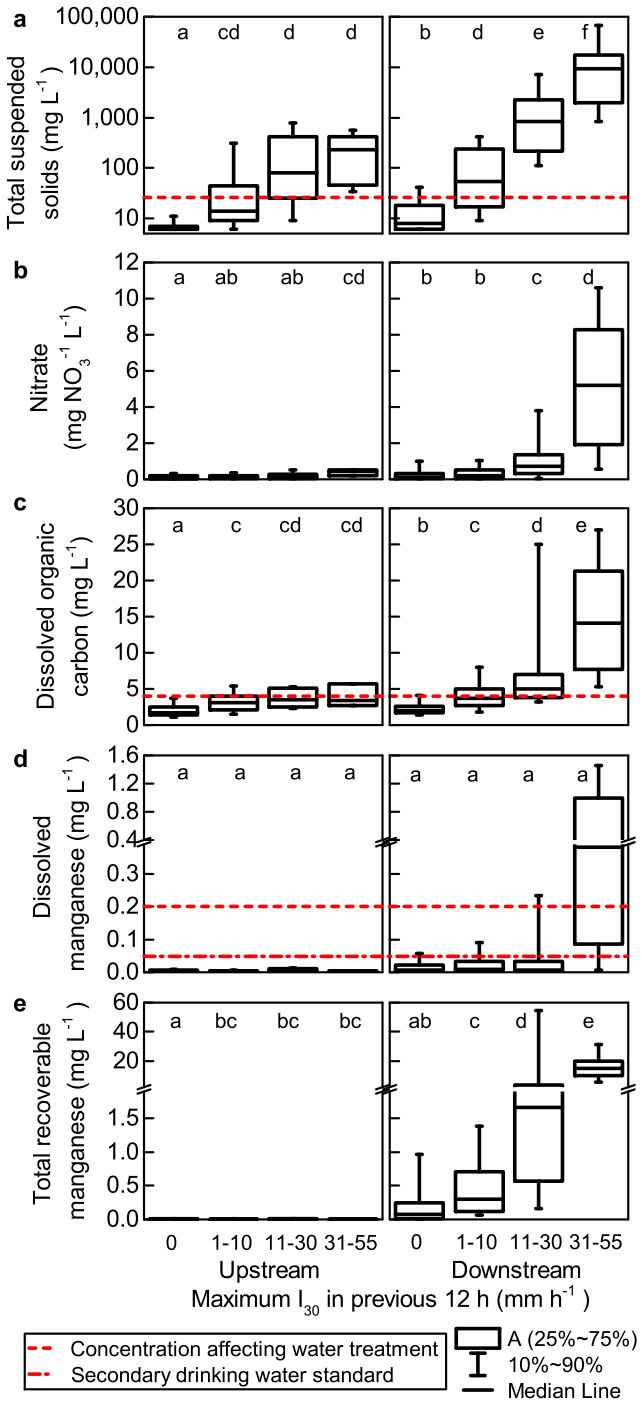

Figure 4. (a)–(e) Constituent concentrations in Fourmile Creek within 12 h of identified maximum 30 min rainfall intensity (I_{30}) for 2011–2013. Upstream includes all samples from sites US1 and US2; downstream includes all samples from DS1, DS2, and DS3. For all sites, maximum I_{30} is from an upstream rain gage, and for sites DS1, DS2, and DS3 the maximum I_{30} is also within the burned area. Dashed lines indicate levels that affect water treatment (see figure 3 caption). Different letters indicate statistically different distributions; $p < 0.05$ using Kruskal–Wallis test (Hollander and Wolfe 1999); see table S2 for more details.

the period before the wildfire, resulting in greater geochemical response.

4.2. Annual runoff and constituent yields after wildfire and the role of storms, snowmelt, and delayed wildfire effects

Annual yields of TSS, NO_3^-, and total recoverable Mn were higher at all sites downstream of the burned area compared to upstream for three years after the Fourmile Canyon fire. For the first two years, this difference, as shown in figure 7, was due to increased downstream yield during July–September (JAS). In April–June (AMJ) 2011, the yields of these constituents were similar upstream and downstream due to similar concentrations and discharge at all sites (figure S1, table S4). The majority of annual runoff from the

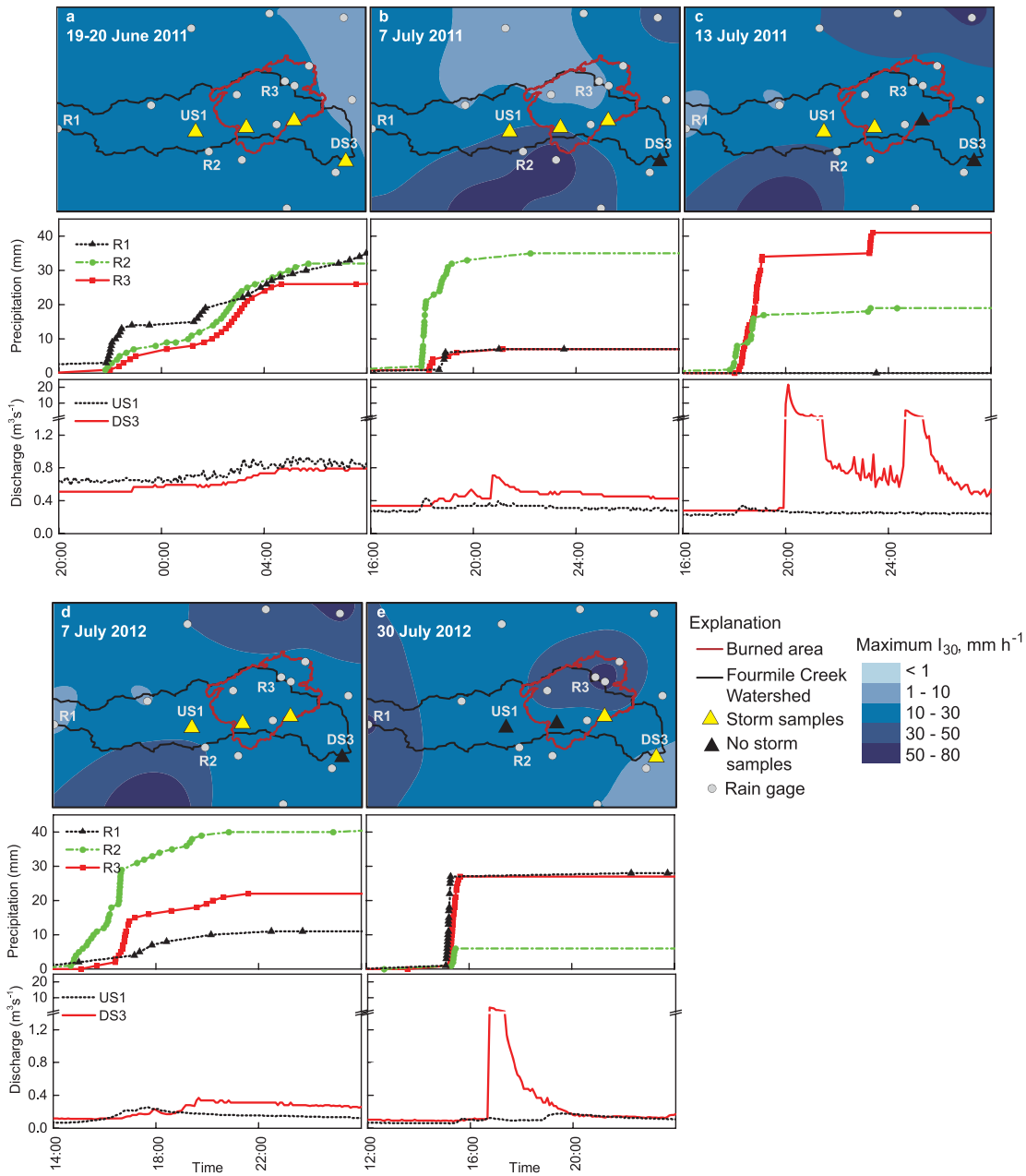

Figure 5. Maps of maximum 30 min rainfall intensity (I_{30}) and corresponding rainfall and stream discharge for select storms. Rainfall intensity could not be estimated in the western edge of the watershed due to lack of tipping-bucket rain gages.

Fourmile Creek Watershed occurs in AMJ (79% historically; table S5); at the upstream, unburned site, annual yield of all evaluated constituents is similarly greatest in AMJ (including 86% of annual TSS yield in 2011; table S5). Downstream of the burned area, in contrast, most (86–88%) of 2011 TSS yield was exported in JAS, primarily during brief periods in response to rain storms with $I_{30} > 10$ mm h^{-1}; almost half of 2011 TSS yield at DS1 was delivered in two one-hour periods on 7 July (104 t) and 13 July (77 t). In comparison, the largest *daily* load at US1 in 2011 was 1.4 t, or 3% of annual load, and coincided with peak discharge in May.

In contrast to TSS, annual DOC yields decreased downstream (figure 7), similar to runoff (runoff, or discharge per unit area, decreases downstream because a majority of annual runoff is derived from the conveyance of snowmelt from headwater areas; figure 2(b)). Between 71% and 84% of annual DOC yield was exported in AMJ at all sites; therefore, very high but brief increases in DOC concentrations downstream of the burned area during storms did not substantially affect annual yield. Dissolved Mn yields in 2011 were higher upstream of the burned area than two of the three downstream sites, and are likely affected by factors other than wildfire (such as mine discharge).

Annual yields of all constituents except DOC were higher downstream of the burned area than upstream in the second and third year post-wildfire (figure 7),

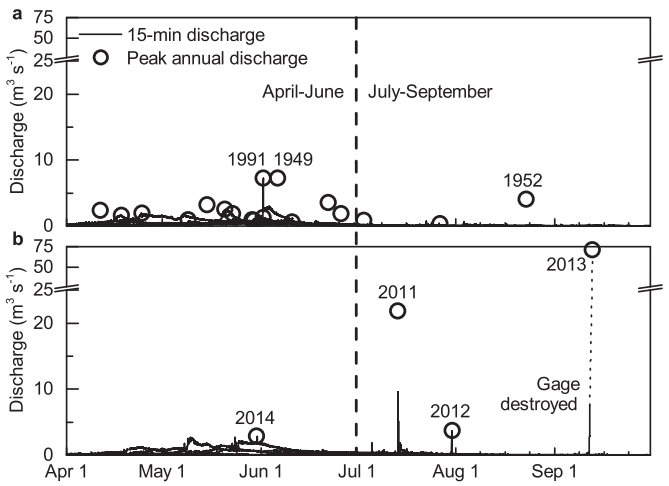

Figure 6. Annual peak discharge and 15 min discharge at site DS3 (USGS streamgaging station 06727500) (a) pre-wildfire (1947, 1949–1953, 1983–1994; 15 min discharge available for 1987–1993 only) and (b) post-wildfire (2011–2014; 15 min data (starting at each hour) were extracted from 5 min data to match intervals available from historical data.

and were again dominated by summer storms. Two July 2012 storms with $I_{30} > 30$ mm h^{-1} in the Gold Run subwatershed delivered 85% of the annual TSS yield at DS3. The most transformative geomorphic event in the three years since the wildfire (and likely for many decades prior) occurred in September 2013 when 210–370 mm rain fell in the Fourmile Creek watershed in 7 days (7 day AEP <0.1%; https://udfcd.onerain.com/home.php). Peak discharge at DS3 was estimated to be 71 m^3 s^{-1}, or 3.3 times greater than the previous peak on 13 July 2011 (figure 6). Numerous debris flows, yet little evidence of deposition, were observed throughout the region (Anderson *et al* 2015), suggesting that most debris was entrained in streamflow and exported out of the area. While sampling was limited during and after this storm, we estimate that an absolute minimum of 6900 t TSS (1.1 t ha^{-1}), and likely much more (because we were not able to sample peak flows) was exported from the Fourmile Creek watershed in the month of September; this is more than had been exported during the entire three years prior.

Interannual climate variation, together with delayed wildfire effects, affected yields of all evaluated constituents during AMJ in 2012 and 2013. Winter-spring precipitation and runoff in these two years represented hydrologic extremes in this watershed. January–June 2012 precipitation at SL (figure 2(a)) was the lowest in 27 y of record, whereas that same period in 2013 was the second highest (http://nadp.sws.uiuc.edu). Discharge in spring 2013, therefore, was substantially higher than in 2012 (figure S1), and was high enough to remobilize stream sediment that had been deposited during post-wildfire JAS storms, whereas in 2012 it was not (we observed the presence of this sediment in the channel through spring 2013). Thus we observed high TSS and total recoverable Mn yields in AMJ 2013 downstream of the burned area (figure 7; table S5). Greatest AMJ (and annual) NO_3^- yields were observed in the third year post-wildfire (table S5), in contrast to several other post-wildfire studies (e.g. Bladon *et al* 2008) and studies cited therein); another study in Colorado, however, also reported a delay (Rhoades *et al* 2011). After disturbance, nitrogen uptake by vegetation is reduced or eliminated, but NO_3^- export can be limited by reduced accumulation due to microbial activity, and/or insufficient water percolation through soil (Vitousek *et al* 1979). Limited vertical percolation during summer 2011 and the winter/spring drought of 2012 may have led to insufficient vertical percolation for NO_3^- export in spring 2012. Vertical percolation during the wet spring of 2013, however, likely led to higher NO_3^- export from soil into the stream at all sites, but greater downstream: AMJ yield was 16 times greater in 2013 than in 2011 at downstream site DS3, compared to two times greater at US1 (figure 7). Dissolved Mn yields in AMJ were 1.4–7.3 times higher in 2013 than in 2011 at downstream sites, but were similar in AMJ in 2011 and 2013 at US1. Manganese is often elevated in wildfire ash (Bodí *et al* 2014) and burned soil (Gonzalez Parra *et al* 1996) and thus elevated stream concentrations and yields may be related to greater water movement through soil in spring 2013 or leaching of channel sediment. We measured elevated Mn concentrations in mine discharge in the watershed (McCleskey *et al* 2012), so increased discharge through mine workings in 2013 could also be a factor.

The maximum TSS and NO_3^- concentrations we observed downstream from the Fourmile Canyon burned area in the first year post-wildfire (68 000 mg TSS L^{-1} and 9.5 mg NO_3^- L^{-1}) fall near or above the upper end of concentrations reported in a review of a range of ecosystems in North America, Australia, and Europe for the same period (11–500 000 mg TSS L^{-1}

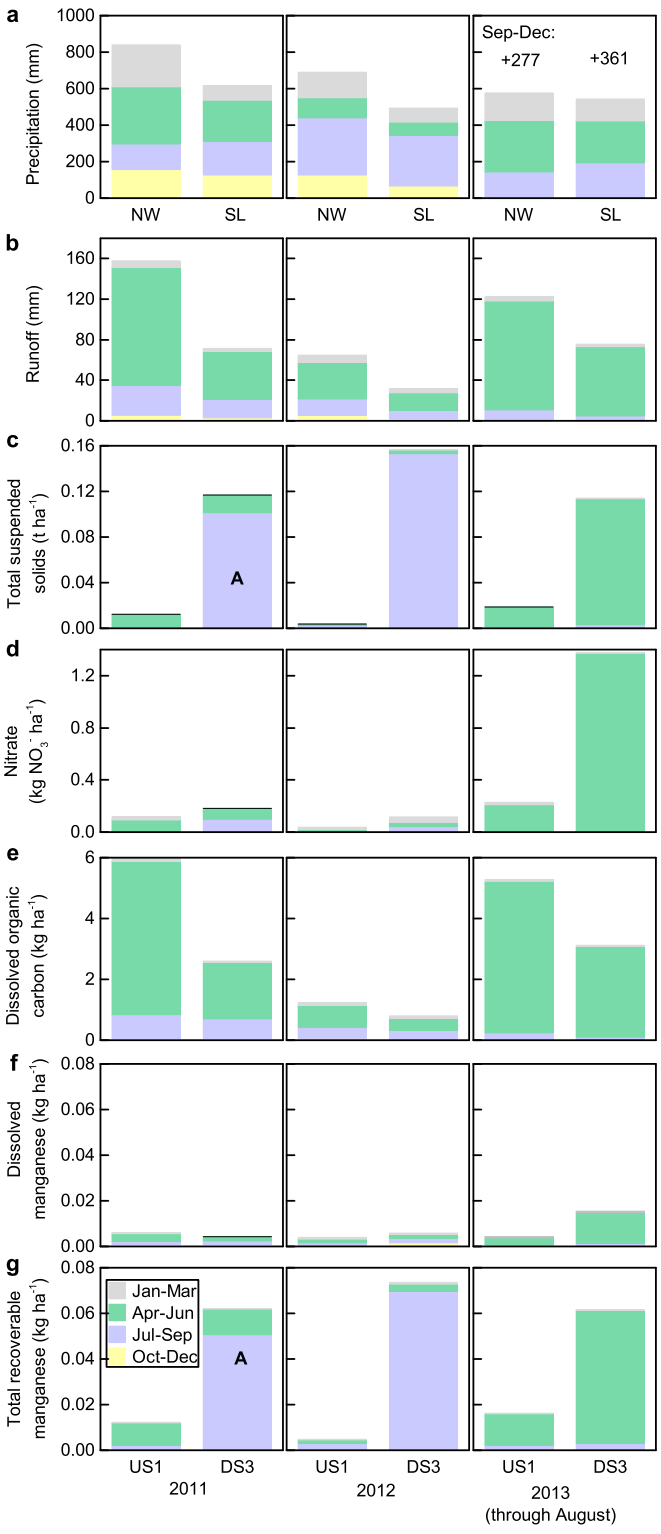

Figure 7. Seasonal contributions of (a) precipitation, (b) runoff (discharge/drainage area), and (c)–(g) constituents at sites US1 and DS3 for the study period. Precipitation at site NW from www.wcc.nrcs.usda.gov and SL from http://nadp.sws.uiuc.edu. A, minimum July–September load because sampler intakes clogged with sediment and burned debris during two storms; 2013 excludes September–December due to destroyed stream gages and site inaccessibility.

and 0.8–5.3 mg L^{-1}; Smith *et al* 2011). However, our yields (0.13 t TSS ha^{-1} and 0.29 kg NO_3^- ha^{-1}) fall within the low range of yields reported in Smith *et al* (2011) (0.017–50 t TSS ha^{-1} and 0.04–13 kg NO_3^- ha^{-1}). Comparison of concentrations and yields for streams draining burned areas is complicated by substantial variations in precipitation regimes, fire severity, ecosystem processes, drainage areas, and sampling and analytical methods (Lane *et al* 2008). Our low yields are probably because our site has relatively low annual precipitation and only 23% of the watershed was burned (largely at low or moderate

severity). In contrast, the highest NO_3^- yields reported in Smith *et al* (2011) were measured in a watershed that was 95% severely burned and received 1658 mm in the first post-wildfire year (Lane *et al* 2006, Lane *et al* 2008).

4.3. Relevance to water providers

Our results show that wildfire and subsequent storms can have short-term (days) and long-term (years) effects on water supplies. For 3.3 years after the Fourmile Canyon fire, water treatment thresholds and/or secondary drinking water standards (Crittenden *et al* 2012) for TSS, DOC, and/or dissolved Mn were exceeded in Fourmile Creek on 56 sampled days downstream of the burned area (site DS2), compared to 20 days upstream (US1) (figure 3). Exceedances of DOC occurred during AMJ in 2011 and 2013 at all sites; higher stream DOC concentrations during snowmelt runoff are expected in the southwestern US (Hornberger *et al* 1994, Nguyen *et al* 2002), and water providers plan accordingly. However, rapid increases in TSS and DOC concentrations during high-intensity rain storms in JAS, when both constituents are typically lower, would present challenges for most water treatment plants. The extremely high concentrations of TSS (up to 120 000 mg L^{-1}) and DOC (up to 71 mg L^{-1}) we observed would decrease water-filtration and pathogen-removal efficiency (Delpla *et al* 2009) and could lead to increased carcinogenic disinfection byproducts upon chlorination (Writer *et al* 2014). Dissolved Mn concentrations exceeded the water-treatment threshold of 0.2 mg L^{-1} on 5 days at DS2, always in response to summer rainstorms with $I_{30} > 10$ mm h^{-1}, and also exceeded the secondary drinking water standard of 0.05 mg L^{-1} on 29 days during those storms and for months afterwards (figure 3). Manganese thresholds or standards were never exceeded at site at US1. Nitrate concentrations, while reaching values up to 12 mg L^{-1} at downstream sites during storms, did not exceed drinking water standards (10 mg L^{-1} NO_3^- as N, or 44 mg L^{-1} NO_3^- as NO_3^-) (Crittenden *et al* 2012).

Increased TSS, NO_3^-, and Mn loads, if delivered to a water-supply reservoir, can lead to long-term impairment of water quantity and quality. Dissolved Mn and particulate-associated Mn have been measured in reservoirs or lakes after wildfire (Taylor *et al* 1993, White *et al* 2006). When incorporated into bottom sediments subjected to chemically reducing conditions, Mn can be released to the overlying water column. Increased nutrient and Mn loads may increase primary productivity, complicating drinking water treatment due to potential increases in algal DOC, phytotoxins, and other taste and odor issues (Brookes *et al* 2008). In addition, the delivery of substantially greater sediment yields after wildfire can shorten reservoir lifetime or require expensive sediment removal. For example, Denver Water spent more than $26 million on water-quality treatment, sediment and debris removal, and related issues after two Colorado wildfires (www.denverwater.org).

The impairment we observed may represent the lower end of potential water-quality consequences in steep, burned watersheds in the southwestern US, particularly those affected by mining and other historical disturbances. The Fourmile Canyon fire burned only 23% of the Fourmile Creek watershed, and only 5% of the watershed was burned at high severity (figure 2(a); table S1). The wildfire occurred near the end of the summer, and no rainstorms with $I_{30} > 10$ mm h^{-1} fell for nine months afterward. No storms with AEP <20% fell in the burned area for nearly two years post-wildfire, yet rain storms with much higher rainfall intensity (50–80 mm h^{-1}, or AEP <2%–10%) fell within a few kilometers of the burned area each summer after the wildfire (figure 5). Finally, no large reservoirs are located immediately downstream of the burned area to trap sediment and nutrients exported during rainstorms (however, decreased quality of water directed into a small local water-supply reservoir required installation of additional treatment equipment; R. de Haas, Pine Brook Water District, written commun., 2012).

Because climate change is projected to increase wildfire frequency and size (Westerling *et al* 2006) and possibly storm frequency and intensity (IPCC 2013), post-wildfire water-quality impacts may be more common in the southwestern US in the future, compounding water supply and quality problems related to projected decreases in runoff and continued population growth (Seager *et al* 2013). Potential adaptation strategies to avoid the introduction of problematic constituents into water-treatment facilities or reservoirs after wildfire vary depending on water distribution systems and water rights portfolios, but could include: filling off-channel water-supply reservoirs prior to the first post-wildfire summer; closing intakes when forecasts indicate a risk of high-intensity summer storms; establishing alternative water supplies; constructing or expanding pre-sedimentation basins; increasing sedimentation capacity at water treatment plants; and developing real-time monitoring networks to provide advanced warning of high-intensity rainfall, flooding, and impaired water quality.

5. Conclusions

Our results demonstrate that high-intensity rainfall is the main driver of elevated post-wildfire TSS, NO_3^-, DOC, and Mn concentrations in the study region. Convective storms, the typical source of high-intensity rainfall, are spatially variable in terms of size, location, and intensity; thus, a dense rain gage network is necessary to estimate rainfall intensity in a burned area. Such a rain gage network, together with storm event sampling and monitoring, are needed to

adequately assess post-wildfire stream response and to model post-wildfire risk to water supplies. Annual yields depend not only on the delivery of constituents to water bodies by high-intensity rainfall in a burned area, but on interannual variations in runoff, which is largely determined by snowmelt from headwater areas that can be upstream of burned areas. The relative importance of snowmelt runoff and summer storms varies among constituents; in this case, rainfall intensity in the burned area was most important for sediment yield, but upstream snowmelt runoff controlled DOC yield. Our findings are applicable to watersheds throughout the southwestern US, where wildfires, high-intensity rainfall, and historical mine waste are common.

Acknowledgments

Support was provided by USGS Water Mission Area (National Research Program), USGS Climate and Land Use Change Mission Area, and NSF grant #0724960, the Boulder Creek Critical Zone Observatory. We thank G Aiken, R Antweiler, K Butler, J Carter, B Ebel, R Jarrett, B Lubenow, J Moody, D Repert, D Roth, R Runkel, R Stallard, D Theune, S Wilson, and D Winter (USGS), USGS Colorado Water Science Center, K Stewart and the Urban Drainage and Flood Control District, US Forest Service, City of Boulder, Boulder County, R De Haas and the Pine Brook Hills Water District, D Dethier, W Ouimet, and the residents of Fourmile Canyon for assistance. Insightful reviews were provided by R F Stallard, S P Anderson, J T Minear, and B A Ebel and two anonymous reviewers.

References

Adams D K and Comrie A C 1997 The North American monsoon *Bull. Am. Meteorol. Soc.* **78** 2197–213

Anderson S, Anderson S and Anderson R 2015 Exhumation by debris flows in the 2013 Colorado front range storm *Geology* **43** 391–4

Barbero R, Abatzoglou J, Steel E A and Larkin N K 2014 Modeling very large-fire occurrences over the continental United States from weather and climate forcing *Environ. Res. Lett.* **9** 124009

Bladon K D, Emelko M B, Silins U and Stone M 2014 Wildfire and the future of water supply *Environ. Sci. Technol.* **48** 8936–43

Bladon K D, Silins U, Wagner M J, Stone M, Emelko M B, Mendoza C A, Devito K J and Boon S 2008 Wildfire impacts on nitrogen concentration and production from headwater streams in southern Alberta's Rocky mountains *Can. J. Forest Res.* **38** 2359–71

Bodí M B, Martin D A, Balfour V N, Santín C, Doerr S H, Pereira P, Cerdà A and Mataix-Solera J 2014 Wildland fire ash: production, composition and eco-hydro-geomorphic effects *Earth-Sci. Rev.* **130** 103–27

Brookes J, Burch M, Hipsey M, Linden L, Antenucci J, Steffensen D, Hobson P, Thorne O, Lewis D and Rinck-Pfeiffer S 2008 *A Practical Guide to Reservoir Management* (Adelaide, South Australia: Water Quality Research Australia Limited)

Brown T C, Hobbins M T and Ramirez J A 2008 Spatial distribution of water supply in the coterminous United States *J. Am. Water Resour. Assoc.* **44** 1474–87

Crittenden J C, Trussell R R, Hand D W, Howe K J and Tchobanoglous G 2012 *MWH's Water Treatment: Principles and Design* (Hoboken, New Jersey: Wiley)

Delpla I, Jung A-V, Baures E, Clement M and Thomas O 2009 Impacts of climate change on surface water quality in relation to drinking water production *Environ. Int.* **35** 1225–33

Dore S, Montes-Helu M, Hart S C, Hungate B A, Koch G W, Moon J B, Finkral A J and Kolb T E 2012 Recovery of ponderosa pine ecosystem carbon and water fluxes from thinning and stand-replacing fire *Glob. Change Biol.* **18** 3171–85

Dudley N and Stolton S 2003 *Running Pure : The Importance of Forest Protected Areas to Drinking Water* (Washington, DC: World Bank/WWF Alliance for Forest Conservation and Sustainable Use)

Emelko M B, Silins U, Bladon K D and Stone M 2011 Implications of land disturbance on drinking water treatability in a changing climate: demonstrating the need for 'source water supply and protection' strategies *Water Res.* **45** 461–72

Gonzalez Parra J, Cala Rivero V and Iglesias Lopez T 1996 Forms of Mn in soils affected by a forest fire *Sci. Total Environ.* **181** 231–6

Higgins R W, Yao Y and Wang X L 1997 Influence of the North American monsoon system on the US summer precipitation regime *J. Clim.* **10** 2600–22

Hollander M and Wolfe D A 1999 *Nonparametric Statistical Methods* (New York: Wiley)

Hornberger G, Bencala K and McKnight D 1994 Hydrological controls on dissolved organic carbon during snowmelt in the Snake River near Montezuma, Colorado *Biogeochemistry* **25** 147–65

Inamdar S P and Mitchell M J 2006 Hydrologic and topographic controls on storm-event exports of dissolved organic carbon (DOC) and nitrate across catchment scales *Water Resour. Res.* **42** W03421

IPCC 2013 *Climate Change 2013: The Physical Science Basis. Contribution of Working Group I to the Fifth Assessment Report of the Intergovernmental Panel on Climate Change* (Cambridge: Cambridge University Press)

Lane P N J, Sheridan G J and Noske P J 2006 Changes in sediment loads and discharge from small mountain catchments following wildfire in south eastern Australia *J. Hydrol.* **331** 495–510

Lane P N J, Sheridan G J, Noske P J and Sherwin C B 2008 Phosphorus and nitrogen exports from SE Australian forests following wildfire *J. Hydrol.* **361** 186–98

Larsen I J, MacDonald L H, Brown E, Rough D, Welsh M J, Pietraszek J H, Libohova Z, de Dios Benavides-Solorio J and Schaffrath K 2009 Causes of post-fire runoff and erosion: water repellency, cover, or soil sealing? *Soil Sci. Soc. Am. J.* **73** 1393–407

McCleskey R B, Writer J H and Murphy S F 2012 Water chemistry data for surface waters impacted by the Fourmile Canyon wildfire, Colorado, 2010–2011 *US Geological Survey Open-File Report 2012–1104* (http://pubs.usgs.gov/of/2012/1104/)

Moody J A and Martin D A 2009 Synthesis of sediment yields after wildland fire in different rainfall regimes in the western United States *Int. J. Wildland Fire* **18** 96–115

Moody J A and Ebel B A 2014 Infiltration and runoff generation processes in fire-affected soils *Hydrol. Process.* **28** 3432–53

Moody J A and Martin R G 2015 Measurements of the initiation of post-wildfire runoff during rainstorms using *in situ* overland flow detectors *Earth Surf. Process. Landf.* **40** 1043–56

Moody J A, Shakesby R A, Robichaud P R, Cannon S H and Martin D A 2013 Current research issues related to post-wildfire runoff and erosion processes *Earth-Sci. Rev.* **122** 10–37

Morton D C, Roessing M E, Camp A E and Tyrrell M L 2003 Assessing the environmental, social, and economic impacts of wildfire (New Haven, CT: Global Institute of Sustainable Forestry)

Murphy S F 2006 State of the watershed: water quality of Boulder Creek Colorado *US Geological Survey Circular 1284* (http://pubs.usgs.gov/circ/circ1284/)

Murphy S F, Verplanck P L and Barber L B 2003 Comprehensive water quality of the Boulder Creek watershed, Colorado, during high-flow and low-flow conditions, 2000 *US Geological Survey Water-Resources Investigations Report* 03-4045 (wwwbrr.cr.usgs.gov/projects/SWC_Boulder_Watershed/)

Murphy S F, McCleskey R B and Writer J H 2012 Effects of flow regime on stream turbidity and suspended solids after wildfire, Colorado Front Range, USA, Wildfire and water quality—Processes, impacts, and challenges *Proceedings of the Conference Held in Banff, Canada, June 2012* IAHS Publ. 354 (Wallingford, UK: IAHS Press)

Neary D G, Ryan K C and Debano L F 2005 Wildland fire in ecosystems: effects of fire on soils and water *USDA Forest Service General Technical Report* RMRS-42

Nguyen M-L, Baker L A and Westerhoff P 2002 DOC and DBP precursors in western US watersheds and reservoirs *J. Am. Water Works Assoc.* **94** 98–112

Perica S, Martin D, Pavlovic S, Roy I, St. Laurent M, Trypaluk C, Unruh D, Yekta M and Bonnin G 2013 *NOAA Atlas 14, Precipitation-Frequency Atlas of the United States* vol 8 (Silver Spring, MD: National Oceanic and Atmospheric Administration) (version 2.0)

Rantz S E *et al* 1982 Measurement and computation of streamflow: volume 1, measurement of stage and discharge *US Geological Survey Water-Supply Paper* 2175 (http://pubs.usgs.gov/wsp/wsp2175/)

Raymond P and Saiers J 2010 Event controlled DOC export from forested watersheds *Biogeochemistry* **100** 197–209

Rhoades C C, Entwistle D and Butler D 2011 The influence of wildfire extent and severity on streamwater chemistry, sediment and temperature following the Hayman Fire, Colorado *International Journal of Wildland Fire* **20** 430–42

Runkel R L, Crawford C G and Cohn T A 2004 *Load Estimator (LOADEST): A FORTRAN program for estimating constituent loads in streams and rivers, US Geological Survey Techniques and Methods 4-A5*

Seager R, Ting M, Li C, Naik N, Cook B, Nakamura J and Liu H 2013 Projections of declining surface-water availability for the southwestern United States *Nat. Clim. Change* **3** 482–6

Smith H G, Sheridan G J, Lane P N, Nyman P and Haydon S 2011 Wildfire effects on water quality in forest catchments: a review with implications for water supply *J. Hydrol.* **396** 170–92

Taylor M J, Shay J M and Hamlin S N 1993 Changes in water-quality conditions in Lexington Reservoir, Santa Clara County, California, following a large fire in 1985 and flood in 1986 *US Geological Survey Water-Resources Investigations Report* 92-4172 (http://pubs.er.usgs.gov/publication/wri924172)

Vitousek P M, Gosz J R, Grier C C, Melillo J M, Reiners W A and Todd R L 1979 Nitrate losses from disturbed ecosystems *Science* **204** 469–74

Weidner E and Todd A 2011 *From the forest to the faucet: Drinking water and forests in the US* (Washington, DC: USDA Forest Service)

Westerling A L, Hidalgo H G, Cayan D R and Swetnam T W 2006 Warming and earlier spring increase western US forest wildfire activity *Science* **313** 940–3

White I, Wade A, Worthy M, Mueller N, Daniell T M and Wasson R 2006 The vulnerability of water supply catchments to bushfires: impacts of the January 2003 wildfires on the Australian Capital Territory *Aust. J. Water Resour.* **10** 179

Williams G P 1989 Sediment concentration versus water discharge during single hydrologic events in rivers *J. Hydrol.* **111** 89–106

Writer J H and Murphy S F 2012 Wildfire effects on source-water quality—lessons from Fourmile canyon fire, Colorado, and implications for drinking-water treatment *US Geological Survey Fact Sheet 2012–3095* (http://pubs.usgs.gov./fs/2012/3095/)

Writer J H, McCleskey R B and Murphy S F 2012 Effects of wildfire on source-water quality and aquatic ecosystems, Colorado Front Range, wildfire and water quality—processes, impacts, and challenges *Proceedings of the Conference Held in Banff, Canada, June 2012* IAHS Publ. 354 (Wallingford, UK: IAHS Press)

Writer J H, Hohner A, Oropeza J, Schmidt A, Cawley K and Rosario-Ortiz F 2014 Water treatment implications after the High Park Wildfire, Colorado *J. Am. Water Works Assoc.* **106** E189–99